



Published in final edited form as:

Neuropharmacology. 2021 October 01; 197: 108746. doi:10.1016/j.neuropharm.2021.108746.

VTA MC3R neurons control feeding in an activity- and sex-dependent manner in mice

Anna I. Dunigan¹, David P. Olson³, Aaron G. Roseberry^{1,2}

¹Department of Biology, Georgia State University, Atlanta, GA 30303, USA;

²Neuroscience Institute, Georgia State University, Atlanta, GA 30303, USA;

³Department of Pediatrics, University of Michigan, Ann Arbor, MI 48109, USA;

Abstract

Increasing evidence indicates that the melanocortin and mesolimbic dopamine (DA) systems interact to regulate feeding and body weight. Because melanocortin-3 receptors (MC3R) are highly expressed in the ventral tegmental area (VTA), we tested whether VTA neurons expressing these receptors (VTA MC3R neurons) control feeding and body weight *in vivo*. We also tested whether there were sex differences in the ability of VTA MC3R neurons to control feeding, as MC3R $-/-$ mice show sex-dependent alterations in reward feeding and DA levels, and there are clear sex differences in multiple DA-dependent behaviors and disorders. Designer receptors exclusively activated by designer drugs (DREADD) were used to acutely activate and inhibit VTA MC3R neurons and changes in food intake and body weight were measured. Acutely altering the activity of VTA MC3R neurons decreased feeding in an activity- and sex-dependent manner, with acute activation decreasing feeding, but only in females, and acute inhibition decreasing feeding, but only in males. These differences did not appear to be due to sex differences in the number of VTA MC3R neurons, the ability of hM3Dq to activate VTA MC3R neurons, or the proportion of VTA MC3R neurons expressing tyrosine hydroxylase (TH). These studies demonstrate an important role for VTA MC3R neurons in the control of feeding and reveal important sex differences in behavior, whereby opposing changes in neuronal activity in male and female mice cause similar changes in behavior.

Keywords

VTA; MC3R; feeding; sex; DREADD

Corresponding Author: Aaron G Roseberry, Neuroscience Institute, Georgia State University, PO Box 5030, Atlanta, GA 30302-5030, Ph: 404-413-5451; Fax: 404-413-5301, aroseberry@gsu.edu.

Author Contributions:

AID performed all experiments. AID & AGR conceived of and designed research, analyzed data, and wrote the manuscript. DPO provided the MC3R-Cre mice.

Publisher's Disclaimer: This is a PDF file of an unedited manuscript that has been accepted for publication. As a service to our customers we are providing this early version of the manuscript. The manuscript will undergo copyediting, typesetting, and review of the resulting proof before it is published in its final form. Please note that during the production process errors may be discovered which could affect the content, and all legal disclaimers that apply to the journal pertain.

Conflicts of Interest: The authors declare no conflicts of interest.

Introduction

The melanocortin system is involved in the control of homeostatic ('need-based') feeding and is comprised of neurons in the arcuate nucleus of the hypothalamus that release the neuropeptides α -melanocyte-stimulating hormone (α -MSH; POMC neurons) or agouti-related peptide (AgRP neurons) as well as the central melanocortin-3 and melanocortin-4 receptors (MC3R and MC4R). Administration of non-specific MCR agonists or extended optogenetic stimulation of POMC neurons decreases food intake and body weight (Aponte et al., 2011; Chen et al., 2000b; Fan et al., 1997; Pierroz et al., 2002), whereas AgRP neuron activation and MCR antagonism stimulates food intake and weight gain (Aponte et al., 2011; Graham et al., 1997; Krashes et al., 2011; Ollmann et al., 1997; Rossi et al., 1998). Although MC4Rs have been extensively studied and play a clear role in the control of feeding, body weight and glucose homeostasis (Butler and Cone, 2002), much less is known about the exact role of MC3Rs. Both MTII, an MC3/4R agonist, and AgRP alter food intake in MC4R^{-/-} mice (Chen et al., 2000b; Marsh et al., 1999; Rowland et al., 2010) demonstrating that MC3Rs can affect feeding. In addition, mice with mutated MC3Rs show altered fat mass, body weight, feeding efficiency, activity levels, fasting-induced refeeding, and food self-administration (Butler et al., 2000; Chen et al., 2000a; Ghamari-Langroudi et al., 2018; Girardet et al., 2017; Lee et al., 2016; Mavrikaki et al., 2016; Renquist et al., 2012). Furthermore, cell-type specific manipulation of MC3R expression in DA or AgRP neurons also alters feeding and food reward (Ghamari-Langroudi et al., 2018; Girardet et al., 2017; Mavrikaki et al., 2016), although these data appear to be contradictory in some cases (i.e. see (Ghamari-Langroudi et al., 2018; Girardet et al., 2017)). Thus, there is evidence that MC3Rs regulate feeding and body weight, but overall, we still have a poor understanding of the exact role that MC3Rs play in the control of energy homeostasis.

In addition to controlling homeostatic feeding, the melanocortin system can also regulate reward-related (hedonic or 'want-based') feeding through its interactions with the mesolimbic DA system (Roseberry et al., 2015). For example, both POMC and AgRP neurons project to the VTA (Dietrich et al., 2012; Dunigan et al., 2020; King and Hentges, 2011), which is the center of the mesolimbic DA system. The VTA is a heterogeneous nucleus that contains DA, glutamatergic, and GABAergic neurons (Nair-Roberts et al., 2008; Yamaguchi et al., 2007) as well as intersectional neural phenotypes containing different combinations of these neurotransmitters (Root et al., 2015; D. H. Root et al., 2014; Stamatakis et al., 2013; Yamaguchi et al., 2011), and MC3Rs are highly expressed in the VTA in both DA and non-DA neurons (Lippert et al., 2014; Roselli-Rehffuss et al., 1993). MC3R^{-/-} mice also show altered food self-administration (Mavrikaki et al., 2016) and altered sucrose preference and changes in DA turnover (Lippert et al., 2014), and our laboratory has shown that intra-VTA injections of melanocortin receptor agonists and antagonists altered both feeding and body weight, and sucrose intake in two-bottle choice tests and self-administration assays (Dunigan et al., 2020; Roseberry, 2013; Shanmugarajah et al., 2017; Yen and Roseberry, 2014). Interestingly the altered sucrose preference and DA turnover observed in the MC3R^{-/-} mouse were sex dependent (Lippert et al., 2014), suggesting that the melanocortin-mesolimbic systems interaction may be sexually dimorphic.

Because MC3Rs are the predominant melanocortin receptor subtype in the VTA (Lippert et al., 2014), VTA neurons expressing this receptor may be a good candidate for a site of interaction between neural circuits controlling homeostatic and reward-based feeding. In these studies, we used transgenic mice expressing Cre recombinase in MC3R neurons (Pei et al., 2019) combined with DREADDs to test whether acute activation or inhibition of VTA MC3R neurons controls feeding and body weight and whether any observed changes in feeding and body weight were sex-dependent.

Materials & Methods

Animals:

Male and female transgenic mice (12–15 weeks old, 18–22 g females and 25–30 g males) expressing Cre recombinase in MC3R neurons ('MC3R-Cre mice') or expressing EYFP in MC3R neurons on a mixed C57/129 background were used in all experiments. MC3R-Cre mice were generously provided by David Olson (University of Michigan, Ann Arbor), and have been previously characterized and validated (Pei et al., 2019; West et al., 2019). Mice expressing EYFP in MC3R neurons were generated by crossing MC3R-Cre mice with Ai3 transgenic mice expressing Cre inducible EYFP (The Jackson Laboratory, stock # 007903). Mice were housed in ventilated polycarbonate Animal Care System cages in a temperature- and humidity-controlled room under a 12:12 light/dark cycle (lights on at 6:00 or 7:00 am) with *ad libitum* food and water throughout the experiment. Mice were group housed until 2 weeks prior to surgery and were housed individually thereafter. All protocols and procedures were approved by the Institutional Animal Care and Use Committee at Georgia State University and conformed to the NIH *Guide for the Care and Use of Laboratory Animals*.

Reagents:

Sterile bacteriostatic saline, ketamine, xylazine, and meloxicam were from Patterson Veterinary Supply, Inc. (Greeley, CO). *Clozapine*-N-oxide (CNO) was from Tocris, Inc. (Minneapolis, MN), and chlorpropamide was from BioVision, Inc. (Milpitas, CA). pAAV-hSyn-DIO-hM3Dq-mCherry and pAAV-hSyn-DIO-hM4Di-mCherry plasmids (Krashes et al., 2011) were direct gifts from Dr. Bryan Roth. pAAV-hSyn-DIO-mCherry (Addgene plasmid # 50459; RRID: Addgene_50459) was a gift from Bryan Roth and was obtained from Addgene. The pHelper and pAAV-RC (2/2) plasmids were a generous gift from Ralph DiLeone. All other reagents were from common commercial sources.

Adeno-associated virus (AAV) preparation:

AAVs were prepared using a triple transfection, helper-free method and were purified as previously described (Hommel et al., 2006). Briefly, HEK293 cells were transfected with equal amounts of pAAV (hM3Dq, hM4Di, or mCherry), pHelper, and pAAV-RC using standard calcium phosphate transfection procedures. Cells were collected ~80 hours post-transfection, resuspended in freezing buffer (150 mM NaCl, 50 mM Tris, pH 8.0), frozen and stored at –80°C until preparation. Cells then underwent 2 freeze-thaw cycles and were incubated with benzonase (50 U/ml final) at 37°C for 30 minutes. The lysate was added to a centrifuge tube containing a 15%, 25%, 40% and 60% iodixanol gradient

and was spun at $184,000 \times g$ (50,000 rpm in a Beckman Type 70Ti rotor) for 3 hours 20 minutes at 10°C. The 40% fraction was collected and exchanged with sterile 1X PBS using Amicon Ultra-15 Centrifugal Filter Unit Concentrators (100 kDalton; Millipore, Inc., Billerica, MA). Viral titers were calculated using the AAV pro Titration Kit (Clontech, Inc.) per the manufacturer's instructions. The final purified viral particles were aliquoted and stored at -80°C, except during use, when they were stored at 4°C.

Stereotaxic surgery:

AAV's were injected into the VTA of MC3R-Cre mice using standard flat-skull stereotaxic techniques. 7–10 week old mice were anesthetized with isoflurane (1–5%) and placed in a stereotaxic apparatus (David Kopf Instruments, Tujunga, CA). The VTA was targeted using the following coordinates (relative to bregma): A/P-3.3, M/L+/-1.32, DV-4.55 and 4.45 from the skull surface, at a 12° angle to the midline. 150 nL of AAV solution was injected bilaterally at each of the two depths (300 nL total/side) at a speed of 100 nl/min using a Nanoliter 2010 microinjector (World Precision Instruments, Sarasota, FL) fitted with glass pipettes with ~30–60 µm diameter tips. The pipettes were left in the brain for 3 minutes following the first injection and 5 minutes following the second injection to allow for AAV diffusion. For pain management, mice received meloxicam (1 mg/kg) at the onset of the surgery and again 24 hours post-surgery. The mice were given 5 weeks for recovery to allow for full DREADD expression prior to the onset of testing.

Food intake and body weight measurement:

Standard laboratory chow (Purina rodent diet #5001, PMI Nutrition International; 3.36 kcal/g) was used in all experiments. Mice were acclimated to eating out of a 10 cm petri dish placed at the bottom of a cage for 1 week prior to the onset of the experiments. For measurement of food intake, mice were given a set amount of food which was then weighed at specific time points to determine the amount of food eaten. For 24-hour food intake measurements, the bedding was sifted to account for spillage whereas spillage was not accounted for during the acute time point measurements due to time constraints and to reduce interference during the experiment. For measurement of body weight, mice were placed in a small box, weighed and then kept in the box for a short duration (<1 min) while the food was weighed before being returned to their cage.

Acute CNO treatment:

Mice were separated into body weight-matched groups prior to surgery and were then randomly injected with one of the three AAVs into the VTA. Following a 5-week recovery period baseline body weight and food intake were measured daily 1 hour before dark onset for 5 days before the first injection and on each intervening non-test day. On test days, body weight and food intake were measured 60 minutes prior to dark onset and all food was removed from the cage. Mice then received an intraperitoneal (IP) injection of CNO (1 mg/kg) or vehicle starting 30 minutes prior to dark onset, and food was re-introduced into the cage 3 minutes before dark onset. Food intake was measured at 1, 2, 3, 4, and 24 hours post-injection and body weight was measured 24 hours post-injection. The animals were allowed 2 days to recover, and the second treatment was administered. Injections were performed in a counterbalanced manner to control for injection order with half of the mice

receiving CNO injections on the first test day and the other half receiving CNO on the second test day. After the termination of the study the mice were euthanized via transcardiac perfusion and brains were collected for *post-hoc* analysis of DREADD expression. CNO was initially dissolved in DMSO, diluted with sterile saline (to 10% DMSO), aliquoted and stored at -20°C until use. Upon use, CNO was diluted to 0.1 mg/mL with sterile saline (1% DMSO final) and used for the injections. The same DMSO/saline mixture (1% DMSO) was used as the vehicle control for all injections. IP injections were done in a volume of 10 $\mu\text{L/g}$ body weight and the injection sides were alternated between each injection. The researcher performing all aspects of the study was blind to the animals' treatment group until all of the data had been collected and DREADD/mCherry expression was confirmed. All mice excluded from the study (see below) were excluded prior to unblinding of the data.

Histological confirmation of DREADD expression:

At the end of all experiments, mice were deeply anesthetized with ketamine/xylazine (93/7 mg/kg) and transcardially perfused with ice cold phosphate buffered saline (PBS) followed by 4% paraformaldehyde. The brains were dissected, post-fixed with 4% paraformaldehyde at 4°C overnight, washed with 1X PBS and incubated in 30% sucrose (in 1X PBS) for 2–3 days until fully saturated with sucrose. The brains were then flash frozen in ethanol/dry ice cooled isopentane and stored at -80°C until sectioning. 40 μm thick coronal sections were collected at 200 μm intervals through the entire VTA on a cryostat, mounted on glass slides and coverslipped using mounting media containing 10% 1,4-diazabicyclo[2.2.2]octane (DABCO). Images were collected at 20x on an Olympus BX41 fluorescent microscope equipped with an Olympus DP73 camera. The images were collected in a grid to visualize the entire VTA and were stitched together post-acquisition using the ImageJ *Stitching* plugin (Preibisch et al., 2009). The number of mCherry positive neurons in the VTA and outside of the VTA were manually quantified using ImageJ *Cell counter* plugin (Schindelin et al., 2012).

Excitatory DREADD (hm3Dq)-mediated activation of c-fos:

Male and female MC3R-Cre mice were injected with AAV-hSyn-DIO-hM3Dq-mCherry or AAV-hSyn-DIO-mCherry into the VTA for analysis of CNO-induced *c-fos* expression. Four to five weeks later, mice received an IP injection of CNO (1mg/kg) or vehicle and were transcardially perfused 2 hours later. Mice used for sex difference analysis received injections of CNO or vehicle near dark onset (at the same time as the experimental injections for the measurement of food intake) and were perfused 2 hours later. The brains were dissected, processed, and the sections were collected as described above. *c-fos* was labeled using standard immunohistochemical (IHC) techniques. In short, brain sections were blocked for 6 hours at room temperature in blocking buffer (5% normal goat serum, 0.2% Triton X-100, 0.1% bovine serum albumin in 1X PBS), washed in 1X PBS for 5 minutes, and were incubated with rabbit anti-*c-fos* antibodies (Cat. # ABE457Millipore, Inc., Billerica, MA) diluted 1:1000 in antibody incubation buffer (0.2% Triton X-100, 1% bovine serum albumin in 1X PBS) overnight at 4°C . Sections were washed with 1X PBS 3 times for 5 minutes each and were incubated with Alexa Fluor 488 conjugated goat anti-rabbit antibodies (Catalog # A-11008, Invitrogen, Carlsbad, CA) diluted 1:1000 in antibody incubation buffer for 4 hours at room temperature. Sections were then washed

with 1X PBS 3 times for 5 minutes each, mounted on glass slides and coverslipped with mounting media containing DABCO. Images of VTA sections containing mCherry and Alexa Fluor 488 (c-fos) signals were acquired using a 20x objective with 0.7X zoom on a confocal microscope (LSM 720; Carl Zeiss, Oberkochen, Germany). The numbers of neurons expressing mCherry, c-fos, and those co-expressing mCherry and c-fos were manually quantified using the ImageJ *Cell Counter* plugin (Schindelin et al., 2012).

MC3R expression analysis:

Brains of male and female mice expressing EYFP in MC3R neurons were collected and processed as describe above and neurons expressing TH were labeled using standard immunohistochemical (IHC) techniques (as described above for c-fos) using mouse anti-TH antibodies (Catalog # MAB318, Millipore, Inc., Billerica, MA) diluted 1:1500 followed by Alexa Fluor 594 conjugated goat anti-mouse antibodies (Catalog # A-11032, Invotrogen, Carlsbad, CA) diluted 1:1000 in antibody incubation buffer. Images of the entire VTA (-2.92 mm to -4.16 mm from bregma) were acquired using a 20x objective with 0.7X zoom on a confocal microscope (LSM 720; Carl Zeiss, Oberkochen, Germany) and were stitched for each VTA section using XuvTools v.1.8.0 (Emmenlauer et al., 2009). The numbers of EYFP positive (MC3R) neurons, Alexa Fluor 594 positive (TH) neurons, and co-expressing neurons were quantified for each section using IMARIS v.9.5.1 (Bitplane). Total cell counts, cell counts per each VTA section, and cell counts for rostral (-2.92mm to -3.28mm from bregma), middle (-3.40 to -3.80mm from bregma) and caudal (-3.88 to -4.16mm from bregma) VTA were compared between the two sexes.

Data analysis, statistics, and experimental design:

All data are presented as means \pm SEM with individual data points included in each graph. Data were graphed using IgorPro (Wavemetrics, Inc., Lake Oswego, OR), and statistical analyses were performed using IBM SPSS Statistics for Windows, Version 25.0 (Armonk, NY). Cumulative food intake was analyzed using a general linear model with repeated measures, with group (hM3Dq, hM4Di, mCherry control), treatment (vehicle vs. CNO), time, and sex (male vs. female), as independent variables. Percent decreases in food intake in males vs. females treated with vehicle vs. CNO were analyzed using general linear model with repeated measures with time and sex (male vs. female) as independent variables. All ANOVAs were followed by *post-hoc* tests corrected for multiple comparisons: Sidak. One-way ANOVA analyses were used to make sex comparisons of DREADD-mediated c-fos expression and MC3R expression. A significance level of $p < 0.05$ was set *a priori* for all analyses.

For the behavioral experiments, mice were included in the data analyses only if the following criteria were met: DREADDs were bilaterally expressed in the VTA, the mouse did not have a clearly visible brain lesion at the injection site, and off-target (e.g. outside the VTA) labeling was <15% of the total number of cells labelled. Some individual mice had poor injections with only a few labeled neurons. To ensure that we only included mice with sufficient labeling to produce a behavioral response, we compared the total number of labeled neurons identified in the VTA in an individual mouse to the mean labeling for the group and excluded mice in which the labeling was 1 standard deviation below the group

mean. Using these criteria resulted in exclusion of 47 mice total (7 control, 20 Gq, 20 Gi). To calculate the means for DREADD-expressing neurons, Gi and Gq groups were combined to obtain a common mean since these groups showed similar expression levels. The control group mean was standalone because the mCherry expression in this group was much higher than in the other two groups. These selection criteria were set *a priori*, and all mice were excluded prior to data unblinding and analysis.

The experiments were repeated in 7 independent cohorts of mice, with the size of the cohorts ranging from 9 to 16 mice per cohort. Information on all of the cohorts of mice tested in these studies, including those that were excluded, is provided in Table 1. This information is included for full transparency and reproducibility.

Results

In these studies, we tested whether acute activation or inhibition of VTA MC3R neurons affected feeding and body weight and whether any observed effects were sex-dependent. AAVs expressing the excitatory DREADD, hM3Dq-mCherry, the inhibitory DREADD, hM4Di-mCherry, or the control, mCherry alone, in a Cre-dependent manner were bilaterally injected into the VTA of MC3R-Cre mice (Figure 1A, B) (Pei et al., 2019; West et al., 2019). CNO (1 mg/kg ip) was then used to activate or inhibit VTA MC3R neurons and changes in feeding and body weight were measured. For all experiments, DREADD-mCherry expression was confirmed to be restricted to the VTA for each mouse at the end of the experiment, and mice were excluded from analysis if the injections were unilateral, there were lesions at the injection site, or if there was significant mCherry expression outside the VTA (Table 1). Representative images showing VTA expression of mCherry for each group are shown in Figure 1C–E, and the mCherry expression pattern was consistent with that shown previously for MC3R expression in the VTA (Lippert et al., 2014; West et al., 2019).

Although the ability of DREADDs to excite and inhibit VTA neurons has been previously established through electrophysiology and IHC (Runegaard et al., 2018; Sandhu et al., 2018; Wang et al., 2013), we confirmed hM3Dq's ability to excite VTA MC3R neurons by examining changes in *c-fos* expression following CNO administration. CNO greatly increased *c-fos* in the VTA neurons expressing hM3Dq-mCherry (Figure 1F–G) compared to the VTA neurons from the control mice expressing mCherry (Figure 1H–I). Consistent with a previous report (Wang et al., 2013), we also observed an increase in *c-fos* in the VTA neurons lacking hM3Dq-mCherry, suggesting excitation through local connectivity or circuit network activity (Figure 1G).

We then tested whether acute activation or inhibition of VTA MC3R neurons with CNO (1 mg/kg) at the onset of the dark phase affected home cage chow consumption or body weight. Although there were small reductions in feeding and body weight when all mice were analyzed together (independent of sex) for both activation and inhibition of VTA MC3R neurons, there were no significant differences observed (data not shown). Addition of sex as a variable in the analysis revealed significant sex-specific effects for both activation and inhibition, however, as shown by significant treatment*group*sex and time*treatment*group*sex interactions. *Post-hoc* analyses demonstrated that activation of

VTA MC3R neurons significantly decreased intake in female mice at all time points (Figure 2D) but did not affect the intake in male mice (Figure 2C). In contrast, inhibition of VTA MC3R neurons significantly decreased food intake in male mice but had no effect in females (Figure 2E–F). As expected, there were no effects of CNO in control mice of either sex (Figure 2A–B).

We next conducted a series of experiments to try to identify the potential cause of the sex differences observed in our behavioral experiment. To determine if the observed differences could be due to sex differences in the ability of hM3Dq to activate VTA MC3R neurons, we compared the number of VTA neurons co-expressing hM3Dq and c-fos following CNO or vehicle injection in male (Figure 3A) and female (Figure 3C) mice expressing hM3Dq-mCherry in VTA MC3R neurons. As we observed in the control experiments in Figure 1, CNO increased c-fos in the VTA neurons expressing hM3Dq-mCherry (Figure 3A–D) compared to vehicle injection in both males and females, but there was no difference in the number of VTA MC3R neurons co-expressing c-fos between sexes (Figure 3E). Thus, it appears that these effects were not due to differences in the ability of the Gq DREADD to activate VTA MC3R neurons between sexes.

We next tested whether the number of VTA MC3R neurons that are DA neurons differed between sexes by analyzing the expression of TH in VTA MC3R neurons. Sample VTA sections collected from male and female mice expressing EYFP in MC3R neurons (green) and immunolabeled for TH (red) are shown in Figure 4. MC3R-expressing neurons were found along the rostro-caudal extent of the VTA but were more concentrated in the middle VTA (–3.40mm to –3.64mm from bregma, Figure 4D) in both sexes. There were no differences in the total number of neurons in the VTA that expressed EYFP (data not shown) or the number of MC3R neurons at different locations along the rostro-caudal extent of the VTA between sexes (Figure 4D). There were also no differences in the total number of TH+ neurons or their rostro-caudal distribution between sexes (data not shown). Importantly, the number of VTA MC3R neurons co-expressing TH (Figure 4B) and the number of TH-positive neurons co-expressing MC3Rs (Figure 4C) were not different between the two sexes, although there was some variability between mice, especially in the middle VTA. Among the MC3R positive population, 37 ± 2 , $64 \pm 3\%$, and $52 \pm 4\%$ co-expressed TH in rostral, middle, and caudal sections, respectively, in males and females combined (Figure 4B), whereas $16 \pm 2\%$, $28 \pm 3\%$, and $25 \pm 3\%$ of TH positive neurons co-expressed MC3R in rostral, middle, and caudal sections (Figure 4C). Thus, it appears that the sex differences in the effects of activation and inhibition of VTA MC3R neurons on feeding were not due to differences in the total number VTA MC3R neurons, the total number of TH neurons or the proportion of MC3R neurons co-expressing TH.

Discussion

In these studies, we tested the effects of acute activation and inhibition of VTA MC3R neurons on food intake and body weight and analyzed whether there were sex differences in the responses to changes in VTA MC3R neuron activity. There were interesting and divergent responses to acute VTA MC3R neuron activation and inhibition, with activation decreasing feeding only in females, and inhibition decreasing feeding only in males (Figure

2) demonstrating that VTA MC3R neurons acutely control feeding in an activity- and sex-dependent manner. We also showed that these sex differences in feeding were not due to sex differences in the ability of Gq DREADDs to activate VTA MC3R neurons, the total number of VTA MC3R neurons, or the percentage of VTA MC3R neurons co-expressing TH as a marker for DA neurons.

The most interesting result of these studies was the robust sex difference in the response to acute activation and inhibition of VTA MC3R neurons (Figure 2, 3). To our knowledge, this is the first demonstration that opposing changes in the activity of a specific neuronal population in males and females can cause the same behavioral response (decreased feeding). Although there is sexual dimorphism in the regulation of feeding and energy homeostasis (Asarian and Geary, 2013; Shi et al., 2009) and sex- and estrous cycle-dependent variations in the melanocortin (Hubbard et al., 2019; Stincic et al., 2018) and mesolimbic DA systems (Becker, 2016; Calipari et al., 2017; Morissette and Di Paolo, 1993), sex differences in behavior, including the regulation of feeding and body weight, typically manifest as a difference in the magnitude of the response between sexes rather than responses in opposite directions. For example, deletion of *Sirt 1* (Ramadori et al., 2010) or *STAT3* (Xu et al., 2007) from POMC neurons increases body weight in female but not male mice, while deletion of GABA_B receptors in POMC neurons results in diet-induced obesity in male but not female mice (Ito et al., 2013). In addition, while both male and female MC4R^{-/-} mice have increased body weight, female mice gain more weight than male mice relative to their same sex controls (Huszar et al., 1997). For each of these examples, one sex showed either no change or a reduced increase in weight rather than an opposite reduction in body weight, which is in contrast to the data presented here, where opposite changes in VTA MC3R neuron activity in males and females cause a similar decrease in feeding. Thus, the results presented here are a novel and interesting demonstration of activity and sex-dependent control of behavior by a specific population of neurons.

One potential explanation for these results is that there could be an inverted-U shaped dose-response curve for VTA MC3R neuron activity-mediated control of feeding, in which both males and females are on the peak of the curve, but baseline activity level is greater in females (right side of peak) than in males (left side of peak). Under this scenario, both a decrease in VTA MC3R neuron activity in females (to the left on the curve) and an increase in VTA MC3R neuron activity in males (to the right on the curve) do not alter feeding, as both remain on the peak of the curve, but an increase in neural activity in females (to the right) and a decrease in neural activity in males (to the left) drive both off of the peak of the curve to cause a decrease in feeding. In support of this model, both increases (Cannon et al., 2004; Mikhailova et al., 2016) and decreases (Szczycka et al., 1999; Zhou and Palmiter, 1995) in DA result in a reduction in feeding (i.e. an inverted U response), and the baseline activity of DA neurons is enhanced in estrus females compared to males (Calipari et al., 2017). As ~40–60% of VTA MC3R neurons are DA neurons (Figure 4B and (Lippert et al., 2014)), changes in DA release downstream of alterations in VTA MC3R neuron activity could drive these effects, although this remains to be tested.

Although the model presented above could explain these responses, the mechanisms underlying the sex differences in the acute response to VTA MC3R neuron activation

are unknown, and many causes could be responsible for the sex differences in feeding observed in these studies. These include differences in how VTA MC3R neurons respond to DREADD-mediated activation and inhibition, anatomical differences in VTA MC3R neurons or their circuit connectivity, or difference in gonadal steroid environment or the response to gonadal steroids. From our experiments, male and female VTA MC3R neurons do not appear to have differential responses to CNO treatment as we observed no differences in the ability of CNO to facilitate *c-fos* gene activation via Gq DREADD (Figure 3). Moreover, we did not detect any differences in the number of neurons expressing MC3Rs, TH, or those co-expressing both markers (Figure 4A–C) and saw no differences in the rostro-caudal distribution of MC3R neurons (Figure 4D), TH neurons (data not shown), or co-expressing neurons (data not shown). It also appears unlikely that differences in the circuit connectivity of VTA MC3R neurons would mediate these effects, as we have recently shown that male and female VTA MC3R neurons do not differ in their efferent projections or their afferent inputs (Dunigan et al., 2020).

One potential explanation for the differences observed here is that there could be sex differences in the specific neurotransmitters or combinations of transmitters released from VTA MC3R neurons. Approximately 40–60% of VTA MC3R neurons are DA neurons (Figure 4B and (Lippert et al., 2014)), and the remaining ~40–60% of VTA MC3R neurons lack TH, indicating that they are GABA and/or glutamate neurons. Alterations in VTA GABA (Soden et al., 2020; Stamatakis et al., 2013; Tan et al., 2012; van Zessen et al., 2012) and glutamate (Qi et al., 2016; David H. Root et al., 2014; Wang et al., 2015) neuron activity have been shown to differentially regulate reward- and aversion-associated behaviors. Therefore, we cannot rule out the contribution of GABA or glutamate release from VTA MC3R neurons to these effects. Additionally, many different intersectional phenotypes of VTA neurons exist including DA neurons that co-release glutamate (Hnasko et al., 2010; Zhang et al., 2015) or GABA (Berrios et al., 2016; Kim et al., 2015; Tritsch et al., 2014), and neurons that co-release glutamate and GABA from the same individual neuron (D. H. Root et al., 2014). As the mechanisms controlling release of one neurotransmitter over the other and the dynamics of co-release from these neurons are not understood, it is possible that neurotransmitter release dynamics from VTA MC3R neurons differ in the two sexes and could contribute to sex differences in feeding behavior, but these possibilities will need to be examined in future experiments.

Recently, several molecularly distinct populations of VTA neurons with different projections and behavioral correlates have been identified (Heymann et al., 2020; Khan et al., 2017; Poulin et al., 2018). Our laboratory has previously performed an extensive analysis of VTA MC3R neuron inputs and projections (Dunigan et al., 2020) and it appears that VTA MC3R neurons overlap with some of the previously described populations and differ from others. For example, the dense ventromedial concentration of the VTA MC3R soma and the specific appearance of their lateral septum projections (Dunigan et al., 2020) resemble the previously classified VTA TH+ population co-expressing Neurogenic Differentiation Factor-6 (NEUROD6), transcription factor orthodenticle homeobox 2 (OTX2), CALBINDIN1, and aldehyde dehydrogenase 1a1 (ALDH1A1) (Khan et al., 2017; Poulin et al., 2018). Similarly, both the organizational pattern of neurons expressing MC3R within the VTA as well as the distribution of their projections in the different subdivisions

of NAc appear to overlap with populations of TH+ neurons co-expressing CCK, or another population expressing Tachykinin Receptor 3 (Tacr3), and yet another population co-expressing vGlut2 (Heymann et al., 2020; Poulin et al., 2018). Some of these neural populations have been shown to differentially regulate behavior, but the role of any of these populations in the regulation of feeding is currently not known. Thus, there may be sex differences in the molecular overlap between these neuronal populations with the VTA MC3R neurons that may be responsible for the sex differences in feeding observed in our experiments, but future studies examining the molecular make of VTA MC3R neurons in both sexes will be needed to establish whether such differences exist.

We also cannot rule out the possibility that reproductive hormones contribute to the sex differences observed here, as the mesocorticolimbic system has been shown to be highly sensitive to the effects of reproductive hormones. For example, baseline activity of DA neurons is enhanced during estrus (Calipari et al., 2017) and DA synthesis and turnover are increased (Pasqualini et al., 1995) and striatal DAT density is decreased (McArthur et al., 2007) by estradiol. It is therefore possible that estradiol may affect the responses of VTA MC3R neurons to acute activation or inhibition, including the physiological effects facilitated by melanocortins, resulting in sexually dimorphic behavioral responses. This possibility appears unlikely, however, because the experimental design utilized in these experiments should have caused individual female mice to be in distinct stages of the estrus cycle on test days. For each individual mouse, test days were separated by 2 days and injections were counterbalanced between mice. Thus, with a ~4-day estrus cycle, the female mice used in this study should have been in distinct stages on test days, and mice were tested in 7 individual cohorts, which makes it unlikely that all female mice in each cohort would have been in the same stage of the estrus cycle during CNO test days. We did not monitor estrus cycle in these studies, however, so it is possible that reproductive hormones could have contributed to the observed differences, although this does not appear likely. Lastly, we cannot rule out the possibility that reproductive hormone-independent, cell-autonomous sex dependent mechanisms contributed to these differential responses. Thus, future experiments will be required to determine the potential role of reproductive hormones in these responses.

Although there were no sex differences in c-fos activation by the Gq DREADD, we cannot entirely rule out the possibility that there were sex differences in the effects of CNO/DREADDs on VTA MC3R neuron activity. Our use of c-fos immunofluorescence as a measure of VTA MC3R neuron activation is a fairly crude measurement that may have missed subtle differences in activity and cannot be used to assess temporal differences in neuronal activation. Moreover, c-fos could not be used to assess Gi DREADD-mediated inhibition because baseline activity was undetectable (see Figure 2Iii). We also did not directly evaluate the Gi DREADD's ability to inhibit VTA MC3R neurons, although the same AAV-DIO-hM4Di-mCherry construct has been previously validated electrophysiologically and behaviorally in mouse VTA TH and DAT-expressing neurons (Runegaard et al., 2018; Sandhu et al., 2018), a population of neurons that overlaps with VTA MC3R neurons. This indicates that the Gi DREADD likely inhibited VTA MC3R neurons in these studies as well, but we cannot rule out sex differences in the ability of the Gi DREADD to inhibit these neurons, although this seems unlikely. Future experiments will be needed to further examine sex differences in VTA MC3R neuron response to Gq

and Gi DREADD-mediated changes in activity, however. Overall, further experiments will be necessary to identify the exact mechanism guiding the sex differences in the feeding response to acute activation and inhibition of VTA MC3R neurons.

In summary, we have demonstrated that VTA MC3R neurons acutely control feeding in a sex- and activity-dependent manner. Overall, these studies suggest that VTA MC3R neurons may be a key site for interaction between homeostatic and hedonic circuits controlling feeding. Furthermore, these studies also reveal important sex differences in behavior and provide novel data showing that opposing changes in neuronal activity in male and female mice can cause similar changes in behavior.

Funding:

Funding for these studies was provided by NIH grant 1R01DK115503 (to AGR) and the Brains and Behavior program at Georgia State University.

Data Availability Statement:

The data that support the findings of this study are available from the corresponding author upon reasonable request.

References

- Aponte Y, Atasoy D, and Sternson SM, 2011. AGRP neurons are sufficient to orchestrate feeding behavior rapidly and without training. *Nat Neurosci.* 14 (3), 351–355. 10.1038/nn.2739 [PubMed: 21209617]
- Asarian L, and Geary N, 2013. Sex differences in the physiology of eating. *American Journal of Physiology-Regulatory Integrative and Comparative Physiology.* 305 (11), R1215–R1267. 10.1152/ajpregu.00446.2012
- Becker JB, 2016. Sex differences in addiction. *Dialogues Clin Neurosci.* 18 (4), 395–402. [PubMed: 28179811]
- Berrios J, Stamatakis AM, Katak PA, McElligott ZA, Judson MC, Aita M, Rougie M, Stuber GD, and Philpot BD, 2016. Loss of UBE3A from TH-expressing neurons suppresses GABA co-release and enhances VTA-NAc optical self-stimulation. *Nat Commun.* 710702. 10.1038/ncomms10702 [PubMed: 26869263]
- Butler AA, and Cone RD, 2002. The melanocortin receptors: lessons from knockout models. *Neuropeptides.* 36 (2–3), 77–84. [PubMed: 12359499]
- Butler AA, Kesterson RA, Khong K, Cullen MJ, Pelleymounter MA, Dekoning J, Baetscher M, and Cone RD, 2000. A unique metabolic syndrome causes obesity in the melanocortin-3 receptor-deficient mouse. *Endocrinology.* 141 (9), 3518–3521. 10.1210/endo.141.9.7791 [PubMed: 10965927]
- Calipari ES, Juarez B, Morel C, Walker DM, Cahill ME, Ribeiro E, Roman-Ortiz C, Ramakrishnan C, Deisseroth K, Han MH, et al., 2017. Dopaminergic dynamics underlying sex-specific cocaine reward. *Nat Commun.* 813877. 10.1038/ncomms13877 [PubMed: 28072417]
- Cannon CM, Abdallah L, Tecott LH, During MJ, and Palmiter RD, 2004. Dysregulation of striatal dopamine signaling by amphetamine inhibits feeding by hungry mice. *Neuron.* 44 (3), 509–520. 10.1016/j.neuron.2004.10.009 [PubMed: 15504330]
- Chen AS, Marsh DJ, Trumbauer ME, Frazier EG, Guan XM, Yu H, Rosenblum CI, Vongs A, Feng Y, Cao L, et al., 2000a. Inactivation of the mouse melanocortin-3 receptor results in increased fat mass and reduced lean body mass. *Nat Genet.* 26 (1), 97–102. 10.1038/79254 [PubMed: 10973258]

- Chen AS, Metzger JM, Trumbauer ME, Guan XM, Yu H, Frazier EG, Marsh DJ, Forrest MJ, Gopal-Truter S, Fisher J, et al., 2000b. Role of the melanocortin-4 receptor in metabolic rate and food intake in mice. *Transgenic Res.* 9 (2), 145–154. 10.1023/a:1008983615045 [PubMed: 10951699]
- Dietrich MO, Bober J, Ferreira JG, Tellez LA, Mineur YS, Souza DO, Gao XB, Picciotto MR, Araújo I, Liu ZW, et al., 2012. AgRP neurons regulate development of dopamine neuronal plasticity and nonfood-associated behaviors. *Nat Neurosci.* 15 (8), 1108–1110. 10.1038/nn.3147 [PubMed: 22729177]
- Dunigan AI, Swanson AM, Olson DP, and Roseberry AG, 2020. Whole-brain efferent and afferent connectivity of mouse ventral tegmental area melanocortin-3 receptor neurons. *J Comp Neurol.* 10.1002/cne.25013
- Emmenlauer M, Ronneberger O, Ponti A, Schward P, Griffa A, Filippi A, Nitschke R, Driever W, and Burkhardt H, 2009. XuvTools: free, fast and reliable stitching of large 3D datasets. *J Microsc.* 233 (1), 42–60. 10.1111/j.1365-2818.2008.03094.x [PubMed: 19196411]
- Fan W, Boston BA, Kesterson RA, Hruby VJ, and Cone RD, 1997. Role of melanocortinergic neurons in feeding and the agouti obesity syndrome. *Nature.* 385 (6612), 165–168. 10.1038/385165a0 [PubMed: 8990120]
- Ghamari-Langroudi M, Cakir I, Lippert RN, Sweeney P, Litt MJ, Ellacott KLJ, and Cone RD, 2018. Regulation of energy rheostasis by the melanocortin-3 receptor. *Sci Adv.* 4 (8), eaat0866. 10.1126/sciadv.aat0866
- Girardet C, Mavrikaki MM, Stevens JR, Miller CA, Marks DL, and Butler AA, 2017. Melanocortin-3 receptors expressed in Nkx2.1(+ve) neurons are sufficient for controlling appetitive responses to hypocaloric conditioning. *Sci Rep.* 744444. 10.1038/srep44444 [PubMed: 28294152]
- Graham M, Shutter JR, Sarmiento U, Sarosi I, and Stark KL, 1997. Overexpression of Agt leads to obesity in transgenic mice. *Nat Genet.* 17 (3), 273–274. 10.1038/ng1197-273 [PubMed: 9354787]
- Heymann G, Jo YS, Reichard KL, McFarland N, Chavkin C, Palmiter RD, Soden ME, and Zweifel LS, 2020. Synergy of Distinct Dopamine Projection Populations in Behavioral Reinforcement. *Neuron.* 105 (5), 909–920.e905. 10.1016/j.neuron.2019.11.024 [PubMed: 31879163]
- Hnasko TS, Chuhma N, Zhang H, Goh GY, Sulzer D, Palmiter RD, Rayport S, and Edwards RH, 2010. Vesicular glutamate transport promotes dopamine storage and glutamate corelease in vivo. *Neuron.* 65 (5), 643–656. 10.1016/j.neuron.2010.02.012 [PubMed: 20223200]
- Hommel JD, Trinko R, Sears RM, Georgescu D, Liu ZW, Gao XB, Thurmon JJ, Marinelli M, and DiLeone RJ, 2006. Leptin receptor signaling in midbrain dopamine neurons regulates feeding. *Neuron.* 51 (6), 801–810. 10.1016/j.neuron.2006.08.023 [PubMed: 16982424]
- Hubbard K, Shome A, Sun B, Pontré B, McGregor A, and Mountjoy KG, 2019. Chronic High-Fat Diet Exacerbates Sexually Dimorphic Pomctm1/tm1 Mouse Obesity. *Endocrinology.* 160 (5), 1081–1096. 10.1210/en.2018-00924 [PubMed: 30997487]
- Huszar D, Lynch CA, Fairchild-Huntress V, Dunmore JH, Fang Q, Berkemeier LR, Gu W, Kesterson RA, Boston BA, Cone RD, et al., 1997. Targeted disruption of the melanocortin-4 receptor results in obesity in mice. *Cell.* 88 (1), 131–141. 10.1016/s0092-8674(00)81865-6 [PubMed: 9019399]
- Ito Y, Banno R, Shibata M, Adachi K, Hagimoto S, Hagiwara D, Ozawa Y, Goto M, Suga H, Sugimura Y, et al., 2013. GABA type B receptor signaling in proopiomelanocortin neurons protects against obesity, insulin resistance, and hypothalamic inflammation in male mice on a high-fat diet. *J Neurosci.* 33 (43), 17166–17173. 10.1523/JNEUROSCI.0897-13.2013 [PubMed: 24155320]
- Khan S, Stott SR, Chabrat A, Truckenbrodt AM, Spencer-Dene B, Nave KA, Guillemot F, Levesque M, and Ang SL, 2017. Survival of a Novel Subset of Midbrain Dopaminergic Neurons Projecting to the Lateral Septum Is Dependent on NeuroD Proteins. *J Neurosci.* 37 (9), 2305–2316. 10.1523/JNEUROSCI.2414-16.2016 [PubMed: 28130357]
- Kim JI, Ganesan S, Luo SX, Wu YW, Park E, Huang EJ, Chen L, and Ding JB, 2015. Aldehyde dehydrogenase 1a1 mediates a GABA synthesis pathway in midbrain dopaminergic neurons. *Science.* 350 (6256), 102–106. 10.1126/science.aac4690 [PubMed: 26430123]
- King CM, and Hentges ST, 2011. Relative number and distribution of murine hypothalamic proopiomelanocortin neurons innervating distinct target sites. *PLoS One.* 6 (10), e25864. 10.1371/journal.pone.0025864 [PubMed: 21991375]

- Krashes MJ, Koda S, Ye C, Rogan SC, Adams AC, Cusher DS, Maratos-Flier E, Roth BL, and Lowell BB, 2011. Rapid, reversible activation of AgRP neurons drives feeding behavior in mice. *J Clin Invest.* 121 (4), 1424–1428. 10.1172/JCI46229 [PubMed: 21364278]
- Lee B, Koo J, Yun Jun J, Gavrilova O, Lee Y, Seo AY, Taylor-Douglas DC, Adler-Wailes DC, Chen F, Gardner R, et al., 2016. A mouse model for a partially inactive obesity-associated human MC3R variant. *Nat Commun.* 710522. 10.1038/ncomms10522 [PubMed: 26818770]
- Lippert RN, Ellacott KL, and Cone RD, 2014. Gender-specific roles for the melanocortin-3 receptor in the regulation of the mesolimbic dopamine system in mice. *Endocrinology.* 155 (5), 1718–1727. 10.1210/en.2013-2049 [PubMed: 24605830]
- Marsh DJ, Hollopeter G, Huszar D, Laufer R, Yagaloff KA, Fisher SL, Burn P, and Palmiter RD, 1999. Response of melanocortin-4 receptor-deficient mice to anorectic and orexigenic peptides. *Nat Genet.* 21 (1), 119–122. 10.1038/5070 [PubMed: 9916804]
- Mavrikaki M, Girardet C, Kern A, Faruzzi Brantley A, Miller CA, Macarthur H, Marks DL, and Butler AA, 2016. Melanocortin-3 receptors in the limbic system mediate feeding-related motivational responses during weight loss. *Mol Metab.* 5 (7), 566–579. 10.1016/j.molmet.2016.05.002 [PubMed: 27408780]
- McArthur S, Murray HE, Dhankot A, Dexter DT, and Gillies GE, 2007. Striatal susceptibility to a dopaminergic neurotoxin is independent of sex hormone effects on cell survival and DAT expression but is exacerbated by central aromatase inhibition. *J Neurochem.* 100 (3), 678–692. 10.1111/j.1471-4159.2006.04226.x [PubMed: 17116232]
- Mikhailova MA, Bass CE, Grinevich VP, Chappell AM, Deal AL, Bonin KD, Weiner JL, Gainetdinov RR, and Budygin EA, 2016. Optogenetically-induced tonic dopamine release from VTA-nucleus accumbens projections inhibits reward consummatory behaviors. *Neuroscience.* 33354–64. 10.1016/j.neuroscience.2016.07.006 [PubMed: 27421228]
- Morissette M, and Di Paolo T, 1993. Sex and estrous cycle variations of rat striatal dopamine uptake sites. *Neuroendocrinology.* 58 (1), 16–22. 10.1159/000126507 [PubMed: 8264850]
- Nair-Roberts RG, Chatelain-Badie SD, Benson E, White-Cooper H, Bolam JP, and Ungless MA, 2008. Stereological estimates of dopaminergic, gabaergic and glutamatergic neurons in the ventral tegmental area, substantia nigra and retrorubral field in the rat. *Neuroscience.* 152 (4), 1024–1031. 10.1016/j.neuroscience.2008.01.046 [PubMed: 18355970]
- Ollmann MM, Wilson BD, Yang YK, Kerns JA, Chen Y, Gantz I, and Barsh GS, 1997. Antagonism of central melanocortin receptors in vitro and in vivo by agouti-related protein. *Science.* 278 (5335), 135–138. 10.1126/science.278.5335.135 [PubMed: 9311920]
- Pasqualini C, Olivier V, Guibert B, Frain O, and Leviel V, 1995. Acute stimulatory effect of estradiol on striatal dopamine synthesis. *J Neurochem.* 65 (4), 1651–1657. 10.1046/j.1471-4159.1995.65041651.x [PubMed: 7561861]
- Pei H, Patterson CM, Sutton AK, Burnett KH, Myers MG, and Olson DP, 2019. Lateral Hypothalamic Mc3R-Expressing Neurons Modulate Locomotor Activity, Energy Expenditure, and Adiposity in Male Mice. *Endocrinology.* 160 (2), 343–358. 10.1210/en.2018-00747 [PubMed: 30541071]
- Pierroz DD, Ziotopoulou M, Ungsuan L, Moschos S, Flier JS, and Mantzoros CS, 2002. Effects of acute and chronic administration of the melanocortin agonist MTII in mice with diet-induced obesity. *Diabetes.* 51 (5), 1337–1345. 10.2337/diabetes.51.5.1337 [PubMed: 11978628]
- Poulin JF, Caronia G, Hofer C, Cui Q, Helm B, Ramakrishnan C, Chan CS, Dombeck DA, Deisseroth K, and Awatramani R, 2018. Mapping projections of molecularly defined dopamine neuron subtypes using intersectional genetic approaches. *Nat Neurosci.* 21 (9), 1260–1271. 10.1038/s41593-018-0203-4 [PubMed: 30104732]
- Preibisch S, Saalfeld S, and Tomancak P, 2009. Globally optimal stitching of tiled 3D microscopic image acquisitions. *Bioinformatics.* 25 (11), 1463–1465. 10.1093/bioinformatics/btp184 [PubMed: 19346324]
- Qi J, Zhang S, Wang H-L, Barker DJ, Miranda-Barrientos J, and Morales M, 2016. VTA glutamatergic inputs to nucleus accumbens drive aversion by acting on GABAergic interneurons. *Nat Neurosci.* advance online publication 10.1038/nn.428110.1038/nn.4281 <http://www.nature.com/neuro/journal/vaop/ncurrent/abs/nn.4281.html#supplementaryinformation> <http://www.nature.com/neuro/journal/vaop/ncurrent/abs/nn.4281.html#supplementaryinformation>

- Ramadori G, Fujikawa T, Fukuda M, Anderson J, Morgan DA, Mostoslavsky R, Stuart RC, Perello M, Vianna CR, Nillni EA, et al., 2010. SIRT1 deacetylase in POMC neurons is required for homeostatic defenses against diet-induced obesity. *Cell Metab.* 12 (1), 78–87. 10.1016/j.cmet.2010.05.010 [PubMed: 20620997]
- Renquist BJ, Murphy JG, Larson EA, Olsen D, Klein RF, Ellacott KL, and Cone RD, 2012. Melanocortin-3 receptor regulates the normal fasting response. *Proc Natl Acad Sci U S A.* 109 (23), E1489–1498. 10.1073/pnas.1201994109 [PubMed: 22573815]
- Root DH, Hoffman AF, Good CH, Zhang S, Gigante E, Lupica CR, and Morales M, 2015. Norepinephrine activates dopamine D4 receptors in the rat lateral habenula. *J Neurosci.* 35 (8), 3460–3469. 10.1523/JNEUROSCI.4525-13.2015 [PubMed: 25716845]
- Root DH, Mejias-Aponte CA, Qi J, and Morales M, 2014. Role of Glutamatergic Projections from Ventral Tegmental Area to Lateral Habenula in Aversive Conditioning. *Journal of Neuroscience.* 34 (42), 13906–13910. 10.1523/jneurosci.2029-14.2014 [PubMed: 25319687]
- Root DH, Mejias-Aponte CA, Zhang S, Wang HL, Hoffman AF, Lupica CR, and Morales M, 2014. Single rodent mesohabenular axons release glutamate and GABA. *Nat Neurosci.* 10.1038/nn.3823
- Roseberry AG, 2013. Altered feeding and body weight following melanocortin administration to the ventral tegmental area in adult rats. *Psychopharmacology (Berl).* 226 (1), 25–34. 10.1007/s00213-012-2879-6 [PubMed: 23010797]
- Roseberry AG, Stuhrman K, and Dunigan AI, 2015. Regulation of the mesocorticolimbic and mesostriatal dopamine systems by alpha-melanocyte stimulating hormone and agouti-related protein. *Neuroscience and Biobehavioral Reviews.* 5615–25. 10.1016/j.neubiorev.2015.06.020 [PubMed: 26116876]
- Roselli-Rehffuss L, Mountjoy KG, Robbins LS, Mortrud MT, Low MJ, Tatro JB, Entwistle ML, Simerly RB, and Cone RD, 1993. Identification of a receptor for gamma melanotropin and other proopiomelanocortin peptides in the hypothalamus and limbic system. *Proc Natl Acad Sci U S A.* 90 (19), 8856–8860. [PubMed: 8415620]
- Rossi M, Kim MS, Morgan DG, Small CJ, Edwards CM, Sunter D, Abusnana S, Goldstone AP, Russell SH, Stanley SA, et al., 1998. A C-terminal fragment of Agouti-related protein increases feeding and antagonizes the effect of alpha-melanocyte stimulating hormone in vivo. *Endocrinology.* 139 (10), 4428–4431. 10.1210/endo.139.10.6332 [PubMed: 9751529]
- Rowland NE, Schaub JW, Robertson KL, Andreasen A, and Haskell-Luevano C, 2010. Effect of MTII on food intake and brain c-Fos in melanocortin-3, melanocortin-4, and double MC3 and MC4 receptor knockout mice. *Peptides.* 31 (12), 2314–2317. 10.1016/j.peptides.2010.08.016 [PubMed: 20800636]
- Runegaard AH, Sørensen AT, Fitzpatrick CM, Jørgensen SH, Petersen AV, Hansen NW, Weikop P, Andreasen JT, Mikkelsen JD, Perrier JF, et al., 2018. Locomotor- and Reward-Enhancing Effects of Cocaine Are Differentially Regulated by Chemogenetic Stimulation of Gi-Signaling in Dopaminergic Neurons. *eNeuro.* 5 (3), 10.1523/ENEURO.0345-17.2018
- Sandhu EC, Fernando ABP, Irvine EE, Tossell K, Kokkinou M, Glegola J, Smith MA, Howes OD, Withers DJ, and Ungless MA, 2018. Phasic Stimulation of Midbrain Dopamine Neuron Activity Reduces Salt Consumption. *eNeuro.* 5 (2), 10.1523/ENEURO.0064-18.2018
- Schindelin J, Arganda-Carreras I, Frise E, Kaynig V, Longair M, Pietzsch T, Preibisch S, Rueden C, Saalfeld S, Schmid B, et al., 2012. Fiji: an open-source platform for biological-image analysis. *Nature Methods.* 9 (7), 676–682. 10.1038/nmeth.2019 [PubMed: 22743772]
- Shanmugarajah L, Dunigan AI, Frantz KJ, and Roseberry AG, 2017. Altered sucrose self-administration following injection of melanocortin receptor agonists and antagonists into the ventral tegmental area. *Psychopharmacology (Berl).* 10.1007/s00213-017-4570-4
- Shi H, Seeley RJ, and Clegg DJ, 2009. Sexual differences in the control of energy homeostasis. *Front Neuroendocrinol.* 30 (3), 396–404. 10.1016/j.yfrne.2009.03.004 [PubMed: 19341761]
- Soden ME, Chung AS, Cuevas B, Resnick JM, Awatramani R, and Zweifel LS, 2020. Anatomic resolution of neurotransmitter-specific projections to the VTA reveals diversity of GABAergic inputs. *Nat Neurosci.* 23 (8), 968–980. 10.1038/s41593-020-0657-z [PubMed: 32541962]
- Stamatakis AM, Jennings JH, Ung RL, Blair GA, Weinberg RJ, Neve RL, Boyce F, Mattis J, Ramakrishnan C, Deisseroth K, et al., 2013. A Unique Population of Ventral Tegmental Area

- Neurons Inhibits the Lateral Habenula to Promote Reward. *Neuron*. 80 (4), 1039–1053. 10.1016/j.neuron.2013.08.023 [PubMed: 24267654]
- Stincic TL, Rønnekleiv OK, and Kelly MJ, 2018. Diverse actions of estradiol on anorexic and orexigenic hypothalamic arcuate neurons. *Horm Behav*. 104146–155. 10.1016/j.yhbeh.2018.04.001 [PubMed: 29626486]
- Szczyпка MS, Mandel RJ, Donahue BA, Snyder RO, Leff SE, and Palmiter RD, 1999. Viral gene delivery selectively restores feeding and prevents lethality of dopamine-deficient mice. *Neuron*. 22 (1), 167–178. 10.1016/s0896-6273(00)80688-1 [PubMed: 10027299]
- Tan KR, Yvon C, Turiault M, Mirzabekov JJ, Doehner J, Labouèbe G, Deisseroth K, Tye KM, and Lüscher C, 2012. GABA neurons of the VTA drive conditioned place aversion. *Neuron*. 73 (6), 1173–1183. 10.1016/j.neuron.2012.02.015 [PubMed: 22445344]
- Tritsch NX, Oh WJ, Gu C, and Sabatini BL, 2014. Midbrain dopamine neurons sustain inhibitory transmission using plasma membrane uptake of GABA, not synthesis. *Elife*. 3e01936. 10.7554/eLife.01936 [PubMed: 24843012]
- van Zessen R, Phillips JL, Budygin EA, and Stuber GD, 2012. Activation of VTA GABA neurons disrupts reward consumption. *Neuron*. 73 (6), 1184–1194. 10.1016/j.neuron.2012.02.016 [PubMed: 22445345]
- Wang HL, Qi J, Zhang S, Wang H, and Morales M, 2015. Rewarding Effects of Optical Stimulation of Ventral Tegmental Area Glutamatergic Neurons. *J Neurosci*. 35 (48), 15948–15954. 10.1523/JNEUROSCI.3428-15.2015 [PubMed: 26631475]
- Wang S, Tan Y, Zhang JE, and Luo M, 2013. Pharmacogenetic activation of midbrain dopaminergic neurons induces hyperactivity. *Neurosci Bull*. 29 (5), 517–524. 10.1007/s12264-013-1327-x [PubMed: 23516143]
- West KS, Lu C, Olson DP, and Roseberry AG, 2019. α -MSH increases the activity of MC3R-expressing neurons in the ventral tegmental area. *J Physiol*. 10.1113/JP277193
- Xu AW, Ste-Marie L, Kaelin CB, and Barsh GS, 2007. Inactivation of signal transducer and activator of transcription 3 in proopiomelanocortin (Pomc) neurons causes decreased pomc expression, mild obesity, and defects in compensatory refeeding. *Endocrinology*. 148 (1), 72–80. 10.1210/en.2006-1119 [PubMed: 17023536]
- Yamaguchi T, Sheen W, and Morales M, 2007. Glutamatergic neurons are present in the rat ventral tegmental area. *Eur J Neurosci*. 25 (1), 106–118. 10.1111/j.1460-9568.2006.05263.x [PubMed: 17241272]
- Yamaguchi T, Wang HL, Li X, Ng TH, and Morales M, 2011. Mesocorticolimbic glutamatergic pathway. *J Neurosci*. 31 (23), 8476–8490. 10.1523/JNEUROSCI.1598-11.2011 [PubMed: 21653852]
- Yen HH, and Roseberry AG, 2014. Decreased consumption of rewarding sucrose solutions after injection of melanocortins into the ventral tegmental area of rats. *Psychopharmacology (Berl)*. 10.1007/s00213-014-3663-6
- Zhang S, Qi J, Li X, Wang HL, Britt JP, Hoffman AF, Bonci A, Lupica CR, and Morales M, 2015. Dopaminergic and glutamatergic microdomains in a subset of rodent mesoaccumbens axons. *Nat Neurosci*. 18 (3), 386–392. 10.1038/nn.3945 [PubMed: 25664911]
- Zhou QY, and Palmiter RD, 1995. Dopamine-deficient mice are severely hypoactive, adipsic, and aphagic. *Cell*. 83 (7), 1197–1209. 10.1016/0092-8674(95)90145-0 [PubMed: 8548806]

Highlights:

MC3Rs are important for feeding, but their exact role is poorly understood

We tested whether altering VTA MC3R neuron activity with DREADDs affected feeding

Acute activation decreased feeding, but only in females

Acute inhibition also decreased feeding, but only in males

Thus, VTA MC3R neurons control feeding in an activity- and sex-dependent manner

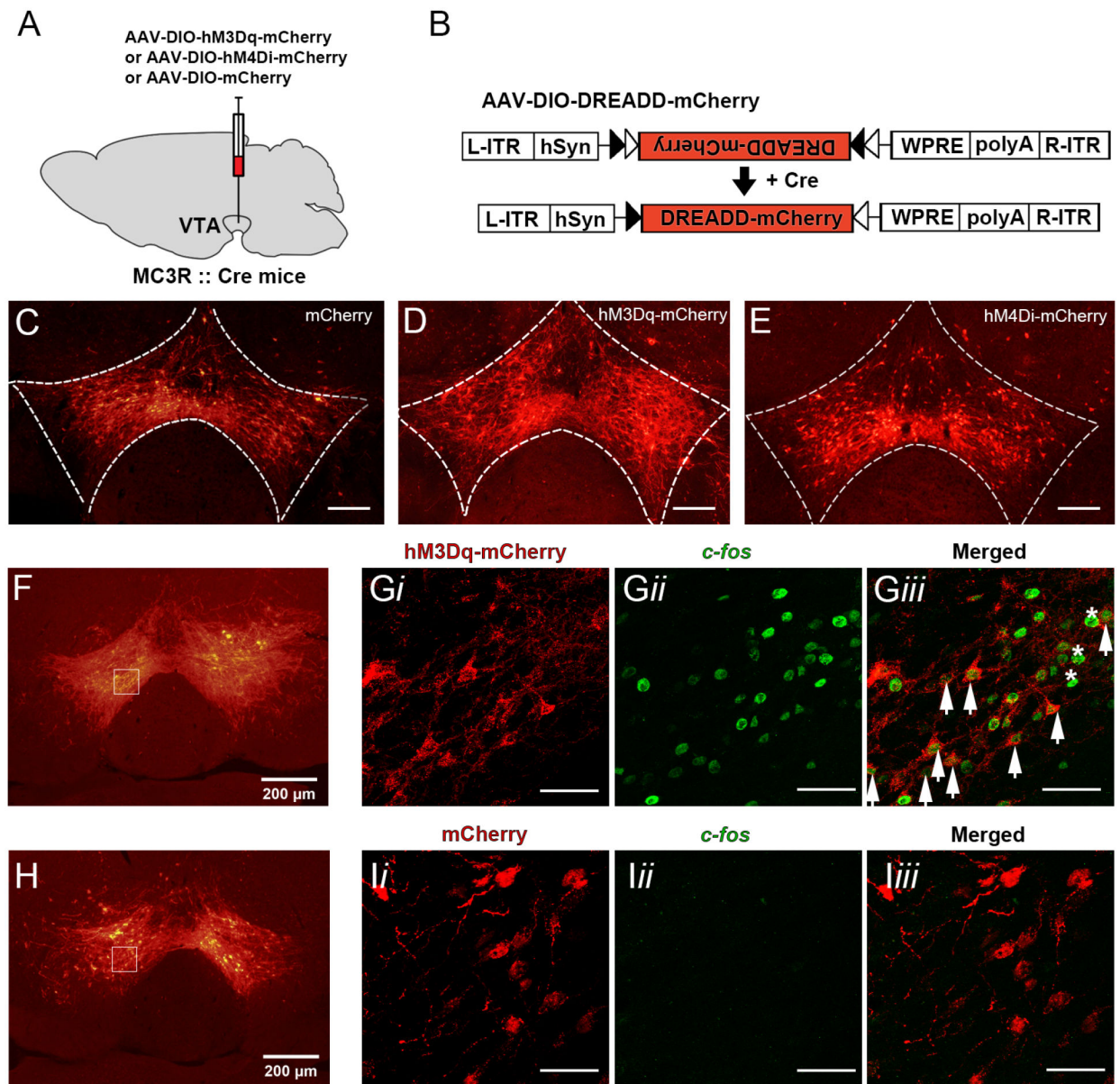


Figure 1: Confirmation of DREADD expression and DREADD-mediated activation of VTA MC3R neurons in MC3R-cre mice. **A.** Graphical representation of AAV-DREADD delivery into the VTA. **B.** General experimental design for AAV-DIO-hM3Dq-mCherry, AAV-DIO-hM4Di-mCherry, and AAV-DIO-mCherry expression. **C-E.** Representative single channel images of VTA sections showing mCherry control (C), hM3Dq-mCherry (D), and hM4Di-mCherry (E) expression in the VTA of MC3R-cre mice. **F-I.** c-fos immunoreactivity two hours after CNO injection (1 mg/kg, i.p.) in VTA neurons expressing hM3Dq-mCherry (F, G) or mCherry control (H, I). Images in F-G $_{ii}$ and H-I $_{ii}$ are of a single channel, whereas G $_{iii}$ and I $_{iii}$ are merged images of red and green channels. Boxes in F and H delineate anatomical location of high magnification images in G and I, respectively. Arrows in G $_{iii}$ identify the cells co-expressing mCherry and c-fos and asterisk exemplify cells expressing

c-fos only. Scale bars: 100 μm (C-E), 50 μm (G, I). L-ITR, left-inverted terminal repeat; hSyn, human synapsin promoter; R-ITR, right-inverted terminal repeat; WPRE, woodchuck hepatitis post-transcriptional regulatory element.

Author Manuscript

Author Manuscript

Author Manuscript

Author Manuscript

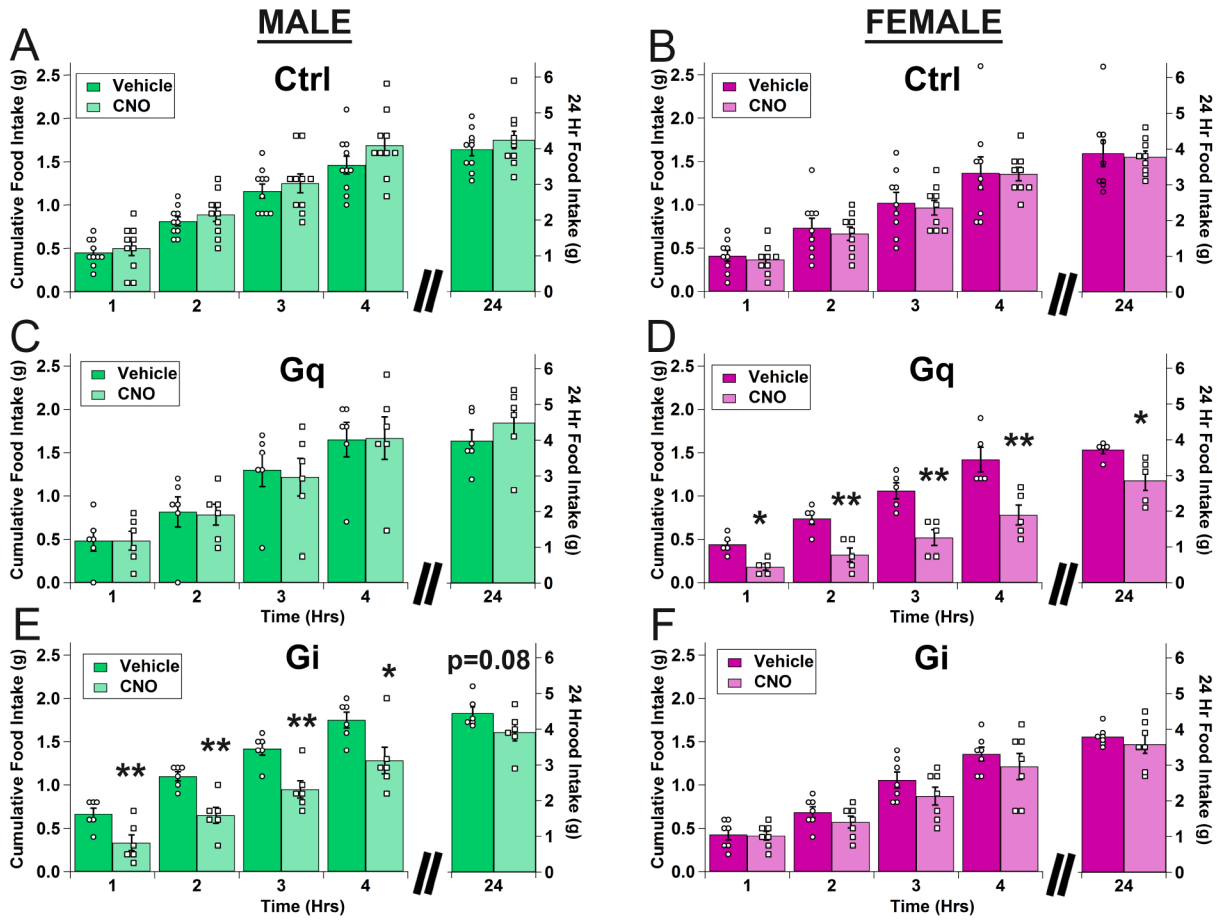


Figure 2: Effects of acute activation and inhibition of VTA MC3R neurons on food intake in males and females. **A-F.** Mean cumulative food intake for male (A, C, E) and female (B, D, F) mice (green = male, magenta = female). **A, B.** Control (mCherry). **C D.** VTA MC3R neuron activation with hM3Dq ('Gq'). **E, F.** VTA MC3R neuron inhibition with hM4Di ('Gi'). Control: n=19 (10 males, 9 females), Gq: n=11 (6 males, 5 females), Gi: n=13 (6 males, 7 females). Open circles are individual data points for vehicle and open squares are individual data points for CNO.* p<0.05 vs. vehicle, **p<0.005 vs. vehicle.

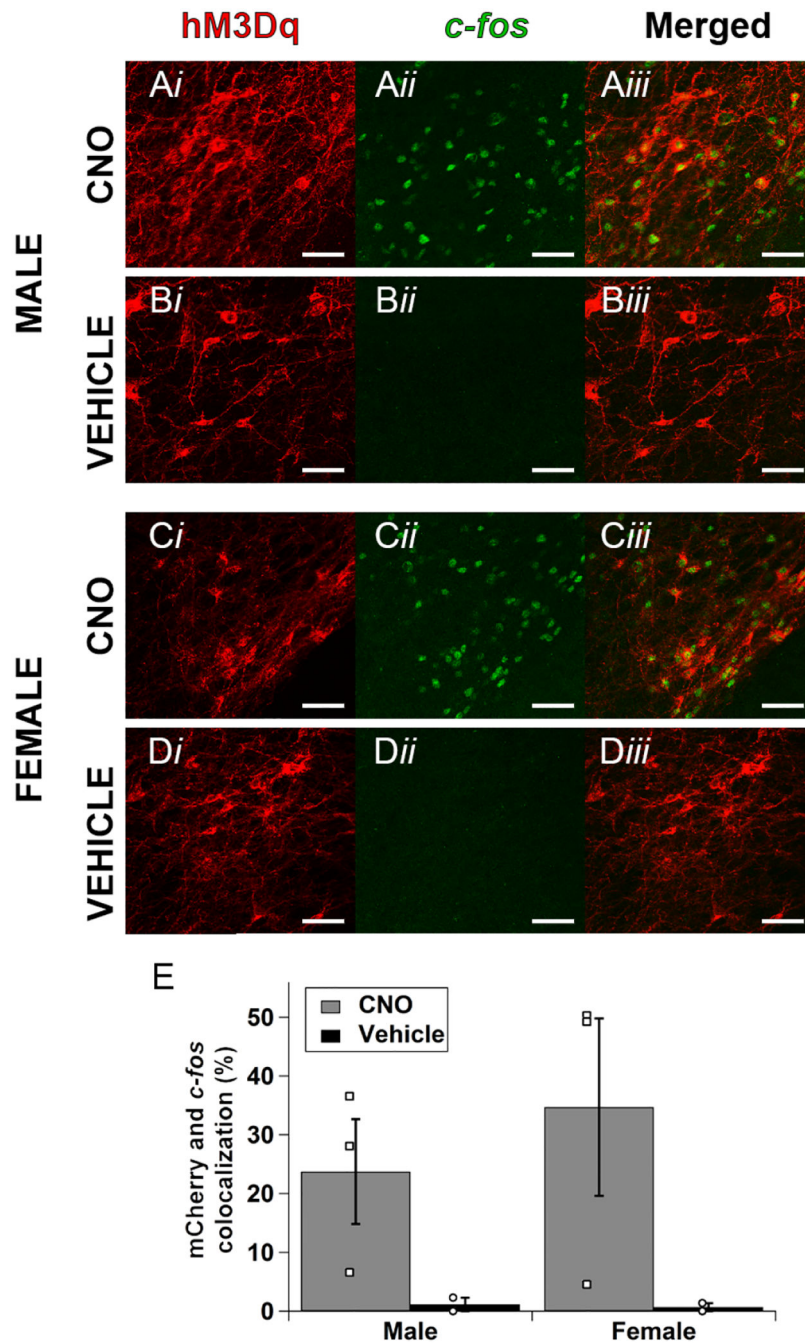


Figure 3: Comparison of CNO-mediated activation of *c-fos* in males and females. **A-D.** Sample images from male (A, B) and female (C, D) mice treated with CNO (A, C) or vehicle (B, D). **E.** Mean mCherry and *c-fos* colocalization in male and female mice treated with CNO (gray) or vehicle (blue) expressed as percent of total mCherry-expressing neurons. Male and female CNO: n=3, male and female vehicle: n=2. Open squares are individual datapoints for CNO and open circles are individual data points for vehicle. Scale bars are 50 μ m.

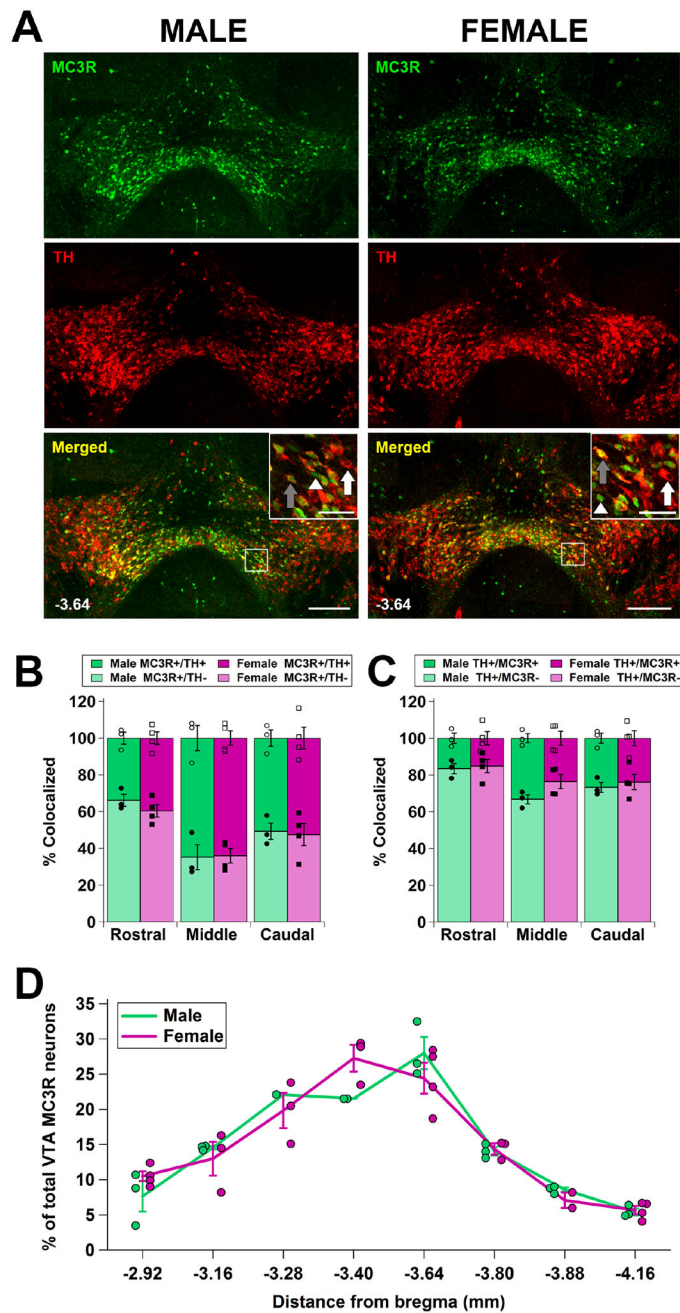


Figure 4: Comparison of neurons co-expressing MC3Rs and TH in males and females. **A.** Sample images from male and female mice immunostained for TH (red) and expressing EYFP in MC3R neurons (green). Insets show higher magnification of the regions in the box and show examples of MC3R+/TH+ (gray arrow), MC3R+/TH- (white arrowhead), and MC3R-/TH+ (white arrow) neurons. **B.** Percentage of MC3R neurons that are positive (dark bar) or negative (light bar) for TH in rostral (-2.92mm to -3.28mm from bregma), middle (-3.40mm to -3.80mm from bregma), and caudal (-3.88mm to -4.16mm from bregma) VTA section of male (green) and female (magenta) mice. **C.** Percentage of TH positive

neurons that do (dark bar) or do not (light bar) contain MC3R-EYFP in rostral, middle, and caudal VTA sections from male (green) and female (magenta) mice. **D.** Rostro-caudal distribution of MC3R-expressing VTA neurons in males (green) and females (magenta). Male: n=3, female: n=4. Open circles and squares (B, C) and colored circles (D) are individual data points. Scale bars: 200 μm (VTA sections), 50 μm (insets).

Table 1:

Detailed description of experimental animals used and excluded in the feeding experiment.

Cohort#	# started	# excluded and reason	# included per sex	# included per group
All animals	90	9- lesions 15- unilateral labeling 8- low labeling 15- >15% off target	22 males 21 females	19 Ctrl 11 Gq 13 Gi
Cohort 1	10	3- lesions 2- unilateral labeling 1- low labeling	1 male 3 females	1 Ctrl 2 Gq 1 Gi
Cohort 2	9	4- lesions 3- >15% off target	1 male 1 female	1 Ctrl 1 Gq
Cohort 3	11	1- lesion 3- unilateral labeling 1- >15% off target	3 males 3 females	3 Ctrl 1 Gq 2 Gi
Cohort 4	13	6- unilateral labeling 1- low labeling 2- >15% off target	3 males 1 female	3 Ctrl 1 Gi
Cohort 5	16	2- unilateral labeling 5- low labeling 2- >15% off target	4 males 3 females	3 Ctrl 2 Gq 2 Gi
Cohort 6	15	1- lesion 1- unilateral labeling 1- low labeling 1- >15% off target	6 males 5 females	4 Ctrl 4 Gq 3 Gi
Cohort 7	16	1- unilateral labeling 6- >15% off target	4 males 5 females	4 Ctrl 1 Gi 4 Gq